Non-WSSUS Vehicular Channel Characterization at 5.2 GHz - Spectral Divergence and Time-Variant Coherence Parameters

Laura Bernadó[1], *Thomas Zemen*[1], *Alexander Paier*[2], *Gerald Matz*[2], *Johan Karedal*[3], *Nicolai Czink*[1], *Charlotte Dumard*[1], *Fredrik Tufvesson*[3], *Martin Hagenauer, Andreas F. Molisch*[3,4], *Christoph F. Mecklenbräuker*[2]

[1]Forschungszentrum Telekommunikation Wien (ftw.), Vienna, Austria
[2]Institut für Nachrichtentechnik und Hochfrequenztechnik, Technische Universität Wien, Vienna, Austria
[3]Department of Electrical and Information Technology, Lund University, Lund, Sweden
[4]Mitsubishi Electric Research Labs, Cambridge, MA, USA
Contact: bernado@ftw.at

Abstract

The scattering environment in vehicle-to-vehicle communication channels at 5.2 GHz changes rapidly. Hence the wide-sense stationary (WSS) uncorrelated scattering (US) assumption for the fading process is valid for short time intervals only. We characterize the spectral divergence of the local scattering function (LSF) sequence in order to assess the non-WSSUS characteristics in different scenarios. We find that the vehicle-to-vehicle channels violate the wide-sense stationarity much stronger than the US assumption. Additionally, we use the LSF to quantify the time dependence of the channel coherence time and bandwidth. Both parameters vary strongly over time depending on the chosen scenario. Furthermore the effect of the antenna radiation pattern on the fading process is quantified, which can cause the strength of a multipath component to change by more than 40 dB in drive-by experiments.

1 Introduction

The wide-sense stationary (WSS) uncorrelated scattering (US) assumption is not valid for the fading process describing a high speed vehicular-to-vehicular radio communication channel. The two constraints that define the WSSUS assumption may be violated. On the one hand, the second order statistic of the fading process changes over time (non-WSS) and, on the other hand, the contributions at different delays can be correlated (non-US) due to reflections on large objects, e.g. a guardrail on the road side. This leads us to characterize the non-WSSUS properties of vehicle-to-vehicle communication channels by means of the local scattering function (LSF) [1].

Contribution of the paper: We reformulate the LSF estimator from [1, 2] in a discrete-time setting suitable for our measurements. Based on the LSF we analyze the spectral divergence in time and frequency to assess the non-WSSUS assumption. Furthermore, an analysis of the time-variant coherence parameters of vehicle-to-vehicle links is provided and the inter-vehicle calibration function is quantified.

Organization of the paper: In Section 2 the LSF estimator is described and in Section 3 the spectral divergence is evaluated in time and frequency. The time-variant coherence parameters are calculated in Section 4 and the influence of the antenna radiation pattern is quantified in Section 5. We conclude this paper in Section 6.

2 Local Scattering Function

A doubly underspread non-WSSUS channel [2] can be seen as an extension of the WSSUS case in the way that the dependency on time and frequency is added to the stochastic analysis. In this paper we use a discrete-time representation of the LSF estimator presented in [1, 2]. The equivalent continuous-time description can be found in [1].

We characterize the wireless communication channel by means of the time-varying transfer function $H(t, f)$ using measurements from the sounding campaign in April 2007 in Lund, Sweden [3]. The channel sounder provides sampled $H[m', q'] = H(m' t_{\mathrm{rep}}, q' B/Q)$, where $t_{\mathrm{rep}} = 307.2\,\mu$s is the repetition time of the channel sounder, $B = 240$ MHz denotes the measurement bandwidth and $Q = 256$ the frequency bins considered in this paper. The samples in the frequency domain are indexed by $q' \in \{0, \ldots, Q-1\}$ and the discrete time-index $m' \in \{0, \ldots, S-1\}$, where $S = 32500$ for an overall measurement period of 10 s.

Note that the LSF $\hat{\mathcal{C}}[m, q; n, p]$ is a sampled version of the continuous time LSF $\hat{\mathcal{C}}(t, f; \tau, \nu)$ in the sense $\hat{\mathcal{C}}[m, q; n, p] = \hat{\mathcal{C}}(m t_{\mathrm{rep}}, qB/Q; n/B, p/(M t_{\mathrm{rep}}))$. Hence the variables $[m, q; n, p]$ correspond to $[t, f; \tau, \nu]$, respectively.

We compute an estimate of the discrete LSF [2, 4]

$$\hat{\mathcal{C}}[m,q;n,p] = \frac{1}{IJMN}\sum_{k=0}^{K-1}\left|\mathcal{H}^{(\boldsymbol{G}_k)}[m,q;n,p]\right|^2 \tag{1}$$

with $n \in \{0,\ldots,N-1\}$ and $p \in \{-M/2,\ldots M/2-1\}$ where

$$\mathcal{H}^{(\boldsymbol{G}_k)}[m,q;n,p] = \sum_{m''=-M/2}^{M/2-1}\sum_{q''=-N/2}^{N/2-1} H[m''-m,q''-q]\boldsymbol{G}_k[m'',q'']\mathrm{e}^{-\mathrm{j}2\pi(pm''-nq'')} \tag{2}$$

using the temporal analysis window length $M = 64$ and the window bandwidth $N = 128$.

The window functions $\boldsymbol{G}_k[m'',q'']$ are well localized within the support region $[-M/2, M/2-1]\times[-N/2, N/2-1]$. Owing to the use of sliding windows, the time and frequency indices m and q for the LSF correspond to the centered sample value of the evaluated window, hence $m \in \{M/2\ldots S-M/2\}$ and $q \in \{N/2\ldots Q-N/2\}$. We apply the discrete time equivalent of the separable transfer function used in [2], $\boldsymbol{G}_k[m'',q''] = u_i[m''+M/2]\tilde{u}_j[q''+N/2]$ where $k = iJ+j$, $i \in \{0\ldots I-1\}$, and $j \in \{0\ldots J-1\}$. The sequences $u_i[m'']$ are chosen as the discrete prolate spheroidal sequences [5] with concentration in the interval $\mathcal{I}_M = \{0\ldots M-1\}$ and bandlimited to $[-I/M, I/M]$, defined as $\sum_{\ell=0}^{M-1}\sin(2\pi I/M(\ell-m''))/(\pi(\ell-m''))u_i[\ell] = \lambda_i u_i[m'']$. The sequences $\tilde{u}_j[q'']$ are defined similarly with concentration in the interval $\mathcal{I}_N$ and bandlimited to $[-J/N, J/N]$.

3 Spectral Divergence

In [4] we use the collinearity measure to assess the similarity of LSF snapshots at different time instants. However the strict positivity of the LSF is not taken into account by such a distance measure. In [6] the spectral divergence measure is introduced as a measure to compare power spectral densities and its usage for fading channels is proposed in [7]. We define the spectral divergence

$$\gamma_t[m_1,m_2] = \log\left(\frac{1}{(MN)^2}\sum_n\sum_p\frac{\hat{\mathcal{C}}^{(t)}[m_1;p,n]}{\hat{\mathcal{C}}^{(t)}[m_2;p,n]}\sum_n\sum_p\frac{\hat{\mathcal{C}}^{(t)}[m_2;p,n]}{\hat{\mathcal{C}}^{(t)}[m_1;p,n]}\right) \tag{3}$$

between two time instants m_1 and m_2, where $\hat{\mathcal{C}}^{(t)}[m;p,n] = \sum_q \hat{\mathcal{C}}[m,q;p,n]$. The spectral divergence in frequency $\gamma_f[q_1,q_2]$ is defined similarly with $\hat{\mathcal{C}}^{(f)}[q;p,n] = \sum_m \hat{\mathcal{C}}[m,q;p,n]$. Note that $\hat{\mathcal{C}}[m,q;n,p]$ is a time-frequency-varying power spectrum and that $\gamma_t[m_1,m_2] \geq 0$ with equality iff $\hat{\mathcal{C}}^{(t)}[m_1;n,p] = \hat{\mathcal{C}}^{(t)}[m_2;n,p]$, which is fulfilled for a WSS fading process. And similarly $\gamma_f \geq 0$ with equality iff $\hat{\mathcal{C}}^{(f)}[q_1;n,p] = \hat{\mathcal{C}}^{(f)}[q_2;n,p]$, which is valid for US.

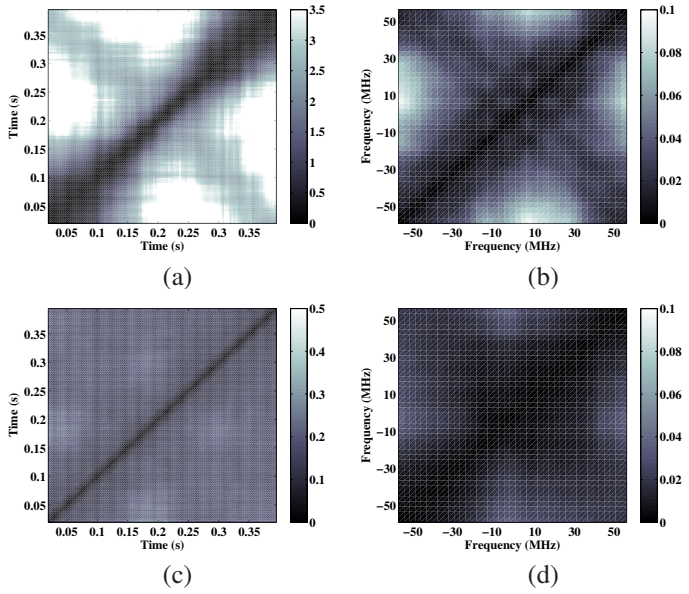

Figure 1: (a) γ_t highway scenario, (b) γ_f highway scenario, (c) γ_t urban scenario, (d) γ_f urban scenario.

We selected the following two scenarios: Highway scenario — two cars driving on the highway in opposite direction at 30.6 m/s (110 km/h). Urban scenario — two cars driving in an urban scenario in the same direction at 13.9 m/s (50 km/h). The normalized power delay profile for both scenarios is shown in Fig. 2.

Figure 1 (a) and (c) show the LSF divergence in time for the highway scenario and the urban scenario, respectively. We zoom into the most extreme conditions for the highway scenario, where the two cars are passing, with length 0.4 s. The divergence is larger in the highway scenario compared to the urban scenario. Please note that the line of sight (LOS) remains almost at a constant delay in the urban scenario (see Fig. 2 (b)). The cross-diagonal in Fig. 1 (a) is due to the geometric symmetry of the scenario (see Fig. 2 (a)). Hence two LSFs have the same delay of the LOS component when $|m_1-m_p| = |m_2-m_p|$ where the two cars are crossing at m_p.

Furthermore, the spectral divergence depending on frequency is shown in Fig. 1 (b) and (d). In that case, we observe that the divergence over frequency is rather small, even though we consider two scenarios with strongly different propagation conditions. Taking into account that the divergence range in frequency is much smaller than in time, we can state that the channels presented in this paper violate the wide-sense stationarity much stronger than the US assumption.

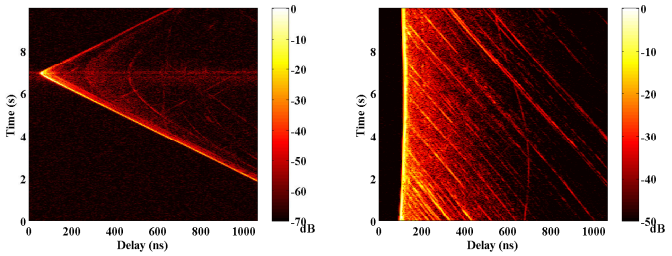

(a) (b)

Figure 2: Normalized power delay profile: (a) highway scenario, (b) urban scenario.

4 Coherence Parameters

In the non-WSSUS case the coherence bandwidth F_c and the coherence time T_c are time variant. In that sense, we define $F_c[m] = 1/\sqrt{\tau^2[m]}$ and $T_c[m] = 1/\sqrt{\nu^2[m]}$ with the delay spread [1]

$$\tau^2[m] \triangleq \frac{\sum_q \sum_n \sum_p (\frac{n}{B})^2 \, \hat{\mathcal{C}}[m,q;n,p]}{\sum_q \sum_n \sum_p \hat{\mathcal{C}}[m,q;n,p]} - \left(\frac{\sum_q \sum_n \sum_p \frac{n}{B} \, \hat{\mathcal{C}}[m,q;n,p]}{\sum_q \sum_n \sum_p \hat{\mathcal{C}}[m,q;n,p]} \right)^2 \tag{4}$$

for time instant m and similarly the instantaneous Doppler spread is given by

$$\nu^2[m] \triangleq \frac{\sum_q \sum_n \sum_p (\frac{n}{Mt_{\text{rep}}})^2 \, \hat{\mathcal{C}}[m,q;n,p]}{\sum_q \sum_n \sum_p \hat{\mathcal{C}}[m,q;n,p]} - \left(\frac{\sum_q \sum_n \sum_p \frac{n}{Mt_{\text{rep}}} \, \hat{\mathcal{C}}[m,q;n,p]}{\sum_q \sum_n \sum_p \hat{\mathcal{C}}[m,q;n,p]} \right)^2 . \tag{5}$$

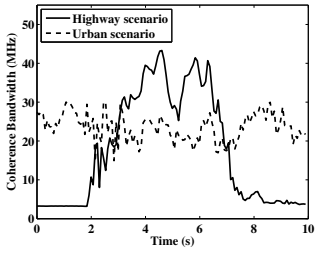

(a)

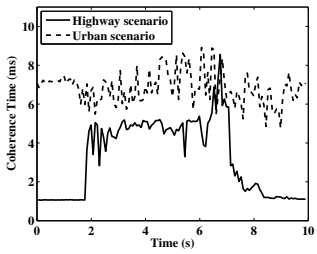

(b)

Figure 3: (a) Coherence bandwidth, (b) Coherence time.

In order to cover the 10 s duration of the measurement, we calculate the LSF with a spacing of 250 samples.

The results in Fig. 3 make clear that the LOS component influences the coherence parameters strongly. In the highway scenario (see Fig. 2 (a)) the LOS component is strong when the two antennas of the considered link, described in Section 5, are facing each other. The coherence bandwidth decreases dramatically after seven seconds, when the two cars are passing each other (see Fig. 3 (a)). From this point on, the two antennas are not facing each other and the LOS component experiences a fast decay of its power. This fast-fading process also decreases the coherence time. In Fig. 3 (b) for the highway scenario, the coherence time decreases strongly after seven seconds, exactly when the antenna link has no direct connection. It is important to notice in Fig. 3 (b) for the highway scenario that the coherence time is largest when the two cars are closest, between six and seven seconds. From zero to two seconds no analysis is possible because the LOS component is outside the maximum delay range of 1000 ns considered in this analysis.

In the urban scenario the strength of the LOS component remains constant over time (see Fig. 2 (b)). Its coherence parameters remain also approximately constant (see Fig. 3 (a) and (b)). The fluctuations occurring throughout the 10s measurement duration correspond to the variation of the reflections produced by the scatterers.

5 Influence of the Antenna Pattern

In these measurement data, the LOS component exhibits large dynamics in power level when both vehicles are passing close by. For the investigations in this paper we consider only the single antenna element No. 3 at both sides

[1] Note that these measures of the coherence time are only approximate; as a matter of fact the coherence bandwidth is related to the delay spread via an uncertainty relationship [8], and similarly for the coherence time / Doppler spread [9].

of the radio link. A short description of the employed antennas is given in [3]. Fig. 4 (a) presents the azimuthal antenna radiation pattern at elevation $0°$ of element No. 3 for the highway scenario. We choose the same antenna element at the Tx and Rx sides because the main lobes are facing towards each other when the vehicles are approaching. Since the antenna is not omnidirectional it will influence the observed Rx power of multipath components strongly. In order to consider this influence we calculated an inter-vehicle calibration function, which includes the impact of *both* antenna radiation patterns (Rx and Tx).

Figure 4 (b) presents this calibration function over time (solid line) as well as the unequalized Rx power (dotted line) and the pathloss-equalized Rx power (dashed line) of the LOS component. This power includes the pathloss calculated with the standard exponential model, considering an attenuation exponent of 1.8, found in [10]. The vehicles are passing after approximately seven seconds. When the vehicles are approaching, the calibration function stays almost constant because there are only small variations in the main lobe. We observe large fluctuations of the calibration function when the vehicles are driving away from each other. This is because of the nulls of the antenna radiation pattern in this angle area (see Fig. 4 (a)). We can see in Fig. 4 (b) that the computed Rx power without the pathloss (dotted line) approximately matches with the calibration function (solid line).

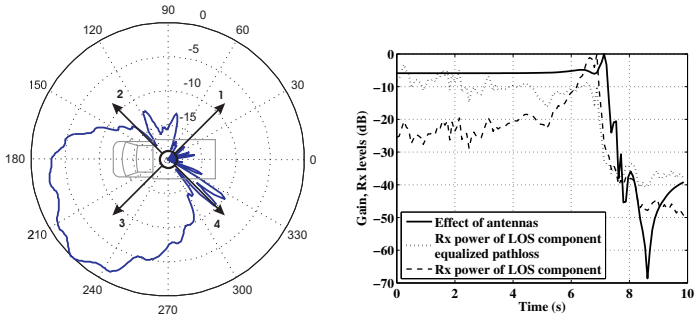

(a) (b)

Figure 4: (a) Antenna radiation pattern for antenna element No. 3, (b) inter-vehicle calibration function

6 Conclusions

We presented a local scattering function (LSF) estimator in time and frequency. Using the spectral divergence of the LSF sequence in time and frequency we showed that the vehicle-to-vehicle channels violate the wide-sense stationarity much stronger than the US assumption. Using the LSF we quantified the time dependence of the channel coherence time and coherence bandwidth. Both parameters vary strongly over time in a drive-by-scenario. Furthermore we showed that the strong variation of the LOS power by more than 40 dB is caused by the antenna radiation pattern. We quantified the inter-vehicle calibration function which fits very well with our measurement results.

References

[1] G. Matz, "On non-WSSUS wireless fading channels," *IEEE Trans. Wireless Commun.*, vol. 4, no. 5, pp. 2465–2478, September 2005.

[2] ——, "Doubly underspread non-WSSUS channels: Analysis and estimation of channel statistics," in *Proc. IEEE Int. Workshop on Signal Processing Advance Wireless Communications (SPAWC)*, Rome, Italy, June 2003, pp. 190–194.

[3] A. Paier, J. Karedal, N. Czink, H. Hofstetter, C. Dumard, T. Zemen, F. Tufvesson, C. F. Mecklenbräuker, and A. F. Molisch, "First results from car-to-car and car-to-infrastructure radio channel measurements at 5.2 GHz," in *International Symposium on Personal, Indoor and Mobile Radio Communications (PIMRC 2007)*, September 2007, pp. 1–5.

[4] A. Paier, T. Zemen, L. Bernadó, G. Matz, J. Karedal, N. Czink, C. Dumard, F. Tufvesson, A. F. Molisch, and C. F. Mecklenbräuker, "Non-WSSUS vehicular channel characterization in highway and urban scenarios at 5.2 GHz using the local scattering function," in *Workshop on Smart Antennas (WSA)*, Darmstadt, Germany, February 2008.

[5] D. Slepian, "Prolate spheroidal wave functions, Fourier analysis, and uncertainty - V: The discrete case," *The Bell System Technical Journal*, vol. 57, no. 5, pp. 1371–1430, May-June 1978.

[6] T. T. Georgiou, "Distances and Riemannian metrics for spectral density functions," *IEEE Trans. Signal Processing*, vol. 55, no. 8, pp. 3995–4003, August 2007.

[7] G. Matz, "Characterization and analysis of doubly dispersive MIMO channels," in *Fortieth Annual Asilomar Conference on Signals, Systems, and Computers*, Pacific Grove, CA, USA, October 2006.

[8] B. Fleury, "An uncertainty relation for WSS processes and its application to WSSUS systems," *Communications, IEEE Transactions on*, vol. 44, no. 12, pp. 1632–1634, December 1996.

[9] M. Molisch, A.F.and Steinbauer, "Condensed parameters for characterizing wideband mobile radio channels," *International Journal of Wireless Information Networks*, vol. 6, pp. 133–154, July 1999.

[10] A. Paier, J. Karedal, N. Czink, H. Hofstetter, C. Dumard, T. Zemen, F. Tufvesson, A. F. Molisch, and C. F. Mecklenbräuker, "Car-to-car radio channel measurements at 5 GHz: Pathloss, power-delay profile, and delay-Doppler spectrum," in *IEEE International Symposium on Wireless Communication Systems (ISWCS 2007)*, October 2007, pp. 224–228.